Indian Journal of Chemistry
Vol. 54A, December 2015, pp. 1459-1465

Synthesis, molecular structure and TD-DFT studies on N'-(pyridine-2-ylmethylene)acetohydrazide nickel(II) complexes

Ram N Patel[a,] *, Yogendra Pratap Singh[a], Yogendra Singh[a] & Raymond J Butcher[b]

[a]Department of Chemistry, APS University, Rewa (MP) 486 003, India
Email: rnp64@ymail.com

[b]Department of Inorganic & Structural Chemistry, Howard University, Washington DC, 22031 USA

Received 10 October 2015; revised and accepted 26 November 2015

Nickel(II) complexes of a Schiff base derived from 2-pyridinecarboxyldehyde and acetylhydrazide, viz., $[Ni(L)_2].(NO_3)_2.H_2O$ (**1**) and $[Ni(HL)(L)].ClO_4.(H_2O)_2$ (**2**) (where L = N'-(pyridine-2-ylmethylene)acetohydrazide), have been synthesized and characterized by physicochemical techniques as well as by single crystal X-ray structural analysis. The supramolecular architecture in both complexes (**1**) and (**2**) are totally guided by complicated H-bondings. The molecular structures and spectral properties of the ligand and the complexes have been explained by DFT and TD-DFT calculations. The electronic excitation energies of these complexes calculated at TD-DFT levels are in agreement with values deduced from the experimental UV-visible spectra.

Keywords: Coordination chemistry, Supramolecular architecture, Schiff bases, Density functional calculations, Nickel

The coordination chemistry of nickel(II) complexes with redox-active ligands represents one of the more promising developments of nickel coordination chemistry with their applications in various areas of science. From the biological point of view, a combination of donor atoms present in many naturally occurring mixed-ligand complexes recognized as enhancing the complex stability[1] is an interesting aspect. The biocatalytic properties of nickel are illustrated by its vigorous role in the global carbon cycle in the catalysing the reversible dehydrogenation of CO and H_2O to CO_2[2]. Nickel is an essential element for methanogenic bacteria, although its function in human organism is still unknown[3].

Synthesis and structural investigation for a series of nickel(II) octahedral complexes have been reported[4] and success has been achieved in generating stable nickel(II) complexes with the help of density functional calculations. The most commonly used approach for engineering the crystal structures of such systems is to employ their hydrogen bonds[5-7]. The quantum chemical studies carried out using the density functional theory have becomes an increasingly useful tool for theoretical studies. The success of DFT is mainly due to the fact that it describes the small molecules more reliably. The results of many studies have indicated that density functional theory is a powerful method for predicting the geometry and harmonic vibration of organic compounds[8-13]. It is a useful method for investigation of large molecules as well[11]. The Cartesian representation of the theoretical force constants are usually computed at optimized geometry by assuming Cs point group symmetry. To show the existence of intramolecular charge transfer (ICT) within a molecular system, energy of the highest occupied molecular orbital (HOMO) and lowest unoccupied molecular orbital (LUMO) levels and the molecular electrostatic surface potential (MESP) energy surface studies are manipulated by DFT[14].

The present work stems from our interest to explore the structural and chelation behavior of N'-(pyridine-2-ylmethylene)acetohydrazide. In the continuation of our work[15-19] on nickel(II) complexes of Schiff base, here we report the synthesis and charactization of N'-(pyridine-2-ylmethylene)-acetohydrazide nickel(II) complexes, viz., complexes $[Ni(L)_2].(NO_3)_2.H_2O$ (**1**) and $[Ni(HL)(L)].ClO_4.(H_2O)_2$ (**2**). The molecular as well as crystalline architectures (supramolecular) of the both complexes (**1**) and (**2**) are guided by complicated H-bonding interactions. Density functional theory calculations complete the characterization of the complexes.

Experimental

Nickel(II) perchlorate hexahydrate, nickel(II) nitrate hexahydrate and N-ethylenediamine were purchased from Aldrich, Qualigens and Across organics respectively. All other chemicals were of synthetic grade and used as received.

The Schiff base was prepared by standard literature procedure[20] and recrystallized from ethanol. The ligand (HL) was synthesized by refluxing 2-pyridin-carboxyldehylde (0.951 g, 10 mmol) and acetylhydrazide (0.740 g, 10 mmol) in ethanol for 4 h at 75 °C, and filtered. The hot solution was cooled slowly and kept at room temperature for slow

evaporation of the solvent. After a week, a light yellow crystalline solid was washed with ethanol and stored in $CaCl_2$ desiccator at RT. Yield: 80%. Anal. Found (%): C, 58.50; H, 5.48; N, 25.70. Calcd (%): C, 58.88; H, 5.56; N, 25.75. IR (KBr disc) 3133 s, 2924 m, 2905 m, 1676 vs, 706 m, 522 m (s, strong; vs, very sharp; m, medium).

$[Ni(L)_2].(NO_3)_2 .H_2O$ (**1**) was prepared as follows: To a MeOH solution (20 mL) of $Ni(NO_3).6H_2O$ (0.365 g, 1.0 mmol), was added a MeOH solution (20 mL) of HL (0.582 g, 2.0 mmol) dissolved with stirring for 30 min at 25 °C. The resulting red solution was allowed to evaporate slowly at room temperature for 3 days. A violet microcrystalline solid deposited was collected by filtration, washed with methanol, and stored in $CaCl_2$ desiccators at room temperature. Anal. (%): Found: C, 36.28; H, 4.15; N, 21.10; Ni, 11.02; Calcd for C_{16} H_{20} N_8: Ni O_9: C, 36.32; H, 4.19; N, 21.18; Ni, 11.09. FAB mass (*m/z*): Obs. (Calcd) 529.08 (385.04). IR (KBr disc) 3538 br, 3133 br, 1650 vs, 1560 s, 746s cm^{-1} (NO_3^-) 1765s (br, broad; s, strong; vs, very sharp; m, medium). μ_{eff} (solid, 298 K): 3.10 μ_B.

$[Ni(HL)(L)].ClO_4.(H_2O)_2$ (**2**) was also prepared similarly, by employing $Ni(ClO_4).6H_2O$ (0.730 g, 2.0 mmol) instead of $NiNO_3.6H_2O$. Anal. (%): Found: C, 31.12; H, 3.50;Cl, 11.40; N, 13.50; Ni, 9.40. Calcd for C_{16} H_{21} Cl N_6 Ni O_8: C, 31.00; H, 3.58; Cl, 11.44; N, 13.56; Ni, 9.47. FAB mass (*m/z*): Obs. (Calcd) 619.89 (384.038). IR (KBr disc) 3538 br, 3133 br, 2924 s. 1624 s, 1652 m, 706 m, 522 m (ClO_4^-) 1104 vs, 863 m, 626 m, 460 vs .μ_{eff} (solid, 298 K): 3.05 μ_B.

Caution! *Although no problems were encountered in this work, perchlorate salts of metal complexes are potentially explosive. They should be synthesized in small quantities and handled with great care.*

FAB mass spectra were recorded on a JEOL SX 102/DA 6000 mass spectrometer using xenon (6 kV, 10 mA) as the FAB gas. The accelerating voltage was 10 kV and the spectra were recorded at room temperature with *m*-nitrobenzoyl alcohol as the matrix. Room temperature magnetic susceptibilities were measured by a Gouy balance using mercury(II) tetrathiocyanato cobaltate(II) as calibrating agent ($\chi_g = 16.44\times10^{-6}$ cgs units). Diamagnetic corrections were estimated from Pascal tables. Ligand field spectra were recorded in solution at 25 ºC on a Shimadzu UV-vis recording spectrophotometer (UV-1601). Infrared (IR) spectra were recorded in KBr medium on a Perkin-Elmer 783 spectrophotometer. Molar conductances were measured using a Systronic conductivity-TDS meter-308. The molecular conductivity of the complexes were measured in DMSO solution (3×10^3 *M*).

Diffraction quality block shaped dark violet crystal of (**1**) and light violet crystal of (**2**) were mounted on a Bruker APEX-II CCD diffractometer equipped with graphite monochromated MoKα radiation (λ = 1.54184 Å for **1** and **2**) from a fine focus sealed tube radiation source. Intensity data were collected at 120 K for (**1**) and (**2**) using φ and ω scan technique. No significant intensity variation was observed during data collection. Multiscan absorption corrections were applied empirically to the intensity values (T_{max} = 0.894 and $T_{min.}$ = 0.717 for **1** and T_{max} = 0.724 and T_{min} = 0.464 for **2**) using SADABS[21]. Data reductions were done by using program Bruker SAINT[22]. The structures were solved by Direct Methods using the program SHELXS-97[23] and refined with full-matrix least-squares based on F2 using program SHELXL-97[23]. All non-hydrogen atoms were refined anisotropically. For both structures hydrogen atoms were first located in the Fourier difference map, then positioned geometrically and allowed to ride on their respective parent. The molecular graphics and crystallographic illustrations for the compounds were prepared using PLATON[24], ORTEP[25], and WinGX [26] program. Crystallographic data and structure refinement parameters for the complexes are summarized in Table 1.

For the computational studies, the input files of the nickel(II) complexes were prepared with Gauss View 5.0.9[27]. All calculations were made using GUASSIAN09 package program[28] by the DFT/B3LYP method with LANL2DZ and 6-31G(d,p) as the standard basic sets. 6-31G(d,p) is a popular polarized basis set which adds p functions to hydrogen atoms in addition to the d functions on heavy atoms, while LANL2DZ is a basis set for post-third-row atoms. In the computational model, the nitrate and perchlorate anion was ignored and the cationic complex was taken into account. The electronic spectrum was predicted by calculating the excitation energy between the states. Electronic spectrum calculations of the complexes were made by using time dependent density functional theory (TD-DFT)/B3LYP method with LANL2DZ basis set in gas phase[29]. The LANL2DZ basis set, with an effective core potential (ECP) was used for Ni [30].

Results and discussion

The ligand (HL) was synthesized by acetyldrazide and 2-pyridine-carboxyldehyde (1:1) in ethanol. All the complexes gave satisfactory elemental analysis and were further characterized by FAB^+ mass spectrometry. The molar conductivity values of 210 and 110 ohm^{-1} cm^{-1} mol^{-1} respectively, indicate the presence of 1:2 and 1:1 electrolyte[31, 32].

The molecular structures of complexes (**1**) and (**2**) show that the nickel(II) centers are in a distorted octahedral geometry with a N_4O_2 donor environment (Fig. 1). Crystal data and structural refinement parameters of the complexes are presented in Table 1. The distortions from ideal octahedral geometry about Ni are of the same extent as those commonly observed for nickel(II) complexes containing multidentate ligands[15, 18, 33]. Individual mean distances and angles compare well with those found for other octahedral nickel(II) complexes involving nitrogen donors[12, 18, 34]. The *cis* and *trans* angles reflect the degree of distortion from ideal octahedral geometry.

(a)

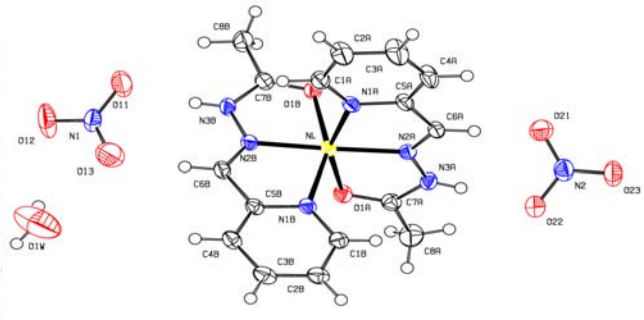

(b)

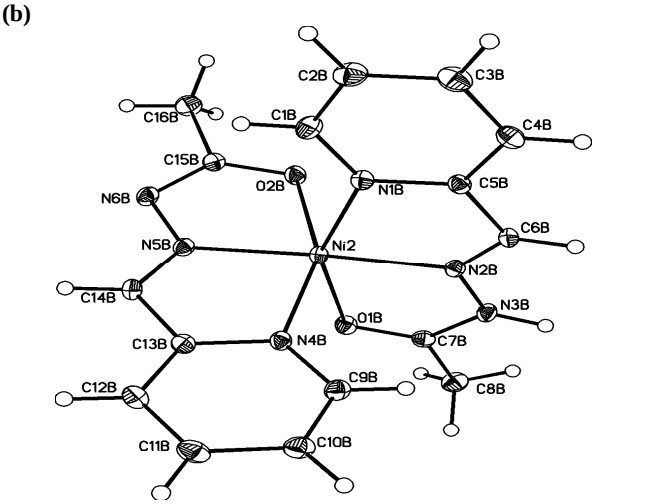

Fig. 1 – ORTEP view of (a) $[Ni(HL)_2].(NO_3)_2.H_2O$ (**1**), and, (b) of $[Ni(HL)(L)]^+$ (**2**).

The five-membered chelate ring is planar in these complexes. These observations are comparable to those found in similar nickel(II) complexes[35, 36].

Complex (**1**) crystallizes in the triclinic space group P-1. Nickel is in a distorted axially compressed octahedron. The ligand (HL) is tridentate via one pyridyl nitrogen, one hydrazone nitrogen and one carbonyl oxygen, thus forming bis chelated structure having four fused five-membered rings. The ligand is coordinated meridionally and would be perpendicular in an idealized octahedron. However, the disposition of the ligands deviates noticeably from perpendicularity as indicated by the decreased value of the *trans* angles (N(2A)–Ni–N(2B)=177.94(7)) and by a significant difference in the values of the inter ligand *cis* angle associated with the same Ni–N(hydrazide) bond [N(2B)-Ni-N(1A)=100.36(8) and N(2B)-Ni-(O(1A)=105.10(7) for the angles involving the N(2A)-Ni-N(1B) = 103.44(7) and 101.60(7) for

Table 1 – Crystal data and structure refinement for (**1**) and (**2**).

Comp.	(**1**)	(**2**)
Emp. formula	$C_{16}H_{20}N_8NiO_9$	$C_{16}H_{21}ClN_6NiO_8$
Formula wt	527.11	519.55
λ (Å)	1.54184	1.54184
Crystal system	Triclinic	Triclinic
Space group	P -1	P -1
a (Å)	7.8454(5)	10.7168(5)
b (Å)	10.6664(9)	13.0287(5)
c (Å)	14.9060(12)	16.0190(7)
α (°)	70.025(7)	75.051(4)
β (°)	86.516(6)	82.354(4)
γ (°)	70.989(7)	88.680(4)
Vol. ($Å^3$)	1106.59(16)	2141.61(17)
Z	2	4
D_{calc} (mg/m^3)	1.582	1.611
μ (Mo Kα) (mm^{-1})	1.867	2.974
F(000)	544	1072
Crystal size (mm^3)	0.51×0.17×0.06	0.3372×0.2287×0.1088
θ range (°)	3.160 to 76.614	2.880 to 76.766
Index range	$-9 \le h \le 8$, $-13 \le k \le 9$, $-18 \le l \le 16$	$-13 \le h \le 13$, $-16 \le k \le 11$, $-20 \le l \le 20$
Refl. collected	9821	20902
Independent refl. [R(int)]	4579 (0.0223)	8907 (0.0271]
Max. and min. transmission	1.00000 and 0.65539	0.787 and 0.560
Data/ restraints/ parameters	4579/ 3/ 323	8907/ 31/ 633
Goodness-of-fit on F^2	1.227	1.037
Final *R* indices [I>2sigma(I)]	*R*1 = 0.0490, w*R*2 = 0.1312	*R*1 = 0.0423, w*R*2 = 0.1149
R indices (all data)	*R*1 = 0.0510, w*R*2 = 0.1329	*R*1 = 0.0494, w*R*2 = 0.1231
Largest diff. peak and hole ($e.Å^{-3}$)	1.830 and -0.662	1.174 and -0.573

the N(2A)-Ni–O(1B) bond]. The Ni–N(hydrazide) bonds (1.9859(18) and 1.9895(19) Å) occupying the equatorial positions are significantly shorter than the Ni–O/N contacts (2.0991(19)–2.1102(16) Å). This difference is indicated by the bis (chelating) mode of the ligands in which Ni–N (hydrazide) bonds appear to be shared by four condensed five-membered chelate rings[34]. The C–N bond length in (**1**) (C(7B)–N(3B) = 1.360(3) and C(7A)–N(3A) = 1.349(3) is inconsistent with partial single-bond character. These factors confirm coordination through the ketonic form. The C–N bond distances of 1.277(3) Å and 1.283(3) Å close to the value of double bond C=N (1.28 Å)[37] confirm the formation of the Schiff base[38]. Selected bond lengths and and bond angles are given in Table S1 (Supplementary data).

The nitrate anions behave as H-bond acceptor towards crystalline water molecules O–H⋯⋯O–N and N(3B)–H⋯⋯O–N (nitrate) resulting in the formation of a 2D undulated layered net-work (supramolecular chain). A view of the packing down axis-b is shown in Fig. 2. The geometrical parameters of H-bonds are collected in Table S2 (Supplementary data).

Complex (**2**) also crystallizes in the triclinic space group P-1. Hydrogen bonding and unit cell packaging diagram is given in Fig. 3.The tridentate ligand in both (HL) and (L) forms is coordinated with nickel(II), as in complex (**1**). The nickel resides in a distorted octahedral environment. Among the Ni-N bond distances, that involving the equatorial azomethine N donor is shorter [Ni(1)-N(2A) and Ni(1)-N(5A) as 1.9783(16) and 2.0027(16) Å], while the Ni-N(py) is [2.1076(16)] is the longest for the sp^3 hybridization of the nitrogen atom [2.1120(16)Å]. Accordingly, the Ni-O2A, *trans* to the Ni-O1A bond is 2.1715(14) and 2.0661(14) Å respectively. This difference is indicated by the bis (chelating) mode of the ligands in which Ni–N (hydrazide) bonds appear to be shared by two condensed five-membered chelate rings. The distortion can be further evidenced from the deviation of the cisoid and transoid angles from the ideal values (Supplementary data, Table S3). The N'-(pyridine-2-ylmethylene)-acetohydrazide ligand has one unit in keto form as indicated by short distance C—O distance 1.238(3)Å and one unit in enol form as indicated by C—O distance 1.270(2) Å. Such an observation has also been made by other workers[34, 18].

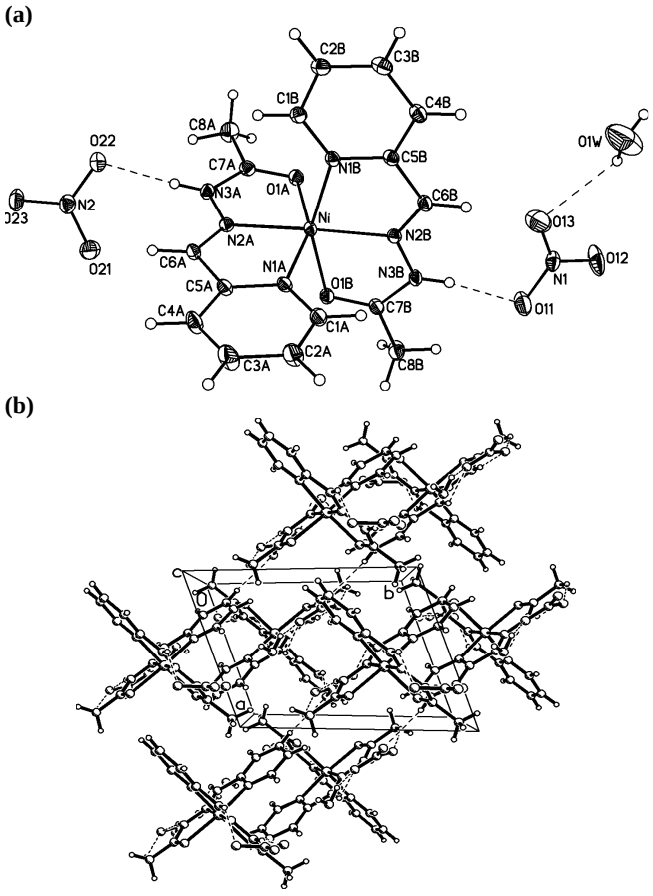

Fig. 2 – (a) Hydrogen bonding, and, (b) unit cell packing diagram with hydrogen bonding for (**1**).

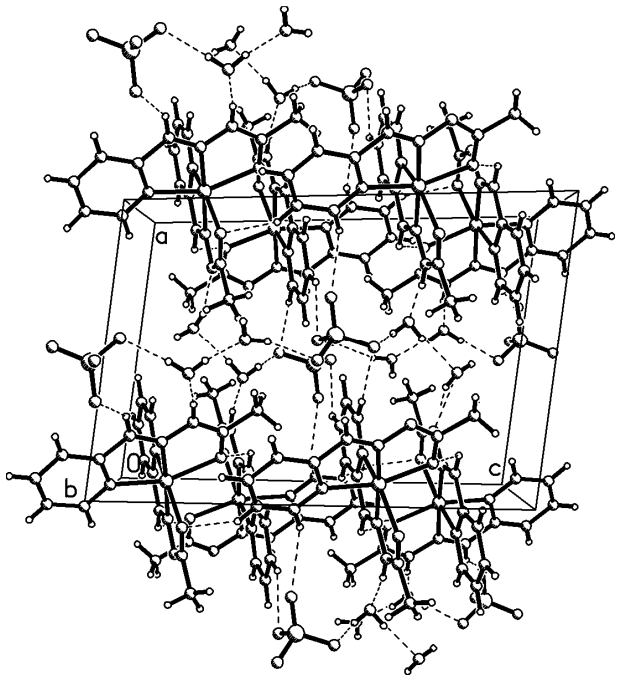

Fig. 3 - Hydrogen bonding and unit cell packaging diagram for (**2**).

Table 2 - TD-DFT calculated excitations approximate assignments for **L**, [Ni(L)].$(NO_3)_2$. H_2O (**1**) and [Ni(HL)(L)].ClO_4.$2H_2O$ (**2**)

Excitation (eV)	Wavelength (nm)	Oscillator strength (*f*)	Major contribution	Expt. wavelength (nm)
N'-(pyridine-2-ylmethylene)acetohydrazide				
2.5382	488.47	0.0000	βHOMO-1→βLUMO (20%) βHOMO→βLUMO (24%)	-
3.0605	405.11	0.0000	βHOMO→βLUMO+1 (22%)	-
3.2110	386.12	0.0000	βHOMO-2→βLUMO (40%)	-
3.2361	383.13	0.0002	βHOMO →βLUMO+1(44%)	-
3.6329	341.28	0.0000	βHOMO-1→βLUMO (22%) βHOMO→βLUMO (21%)	-
3.7992	326.34	0.0013	βHOMO-2→ βLUMO (49%)	320
[Ni(L)].$(NO_3)_2$. H_2O (1)				
0.6984	1380.09	0.0000	βHOMO-1→βLUMO+1 (23%)	
1.0109	1229.58	0.0001	βHOMO→βLUMO+1 (18%)	
1.2336	959.47	0.0020	βHOMO-1→βLUMO (44%)	998
1.4211	861.70	0.0041	βHOMO→βLUMO (14%)	
1.5625	628.54	0.0005	βHOMO→βLUMO+1 (32%) βHOMO→βLUMO+2 (11%)	693
1.7708	578.37	0.0027	βHOMO→βLUMO (45%)	382
[Ni(HL)(L)].ClO_4.$2H_2O$ (2)				
0.3933	1352.59	0.0005	βHOMO→βLUMO (87%)	-
1.0071	1231.12	0.0002	βHOMO→βLUMO (12%) βHOMO→βLUMO +1(51%)	-
1.3410	924.55	0.0007	βHOMO→βLUMO +1(17%) βHOMO→βLUMO +3(48%)	998
1.4270	868.85	0.0003	βHOMO→βLUMO +3(15%)	-
1.6624	745.81	0.0003	βHOMO→βLUMO +1(4%)	680
1.8195	681.41	0.0115	βHOMO→βLUMO +4(94%)	380

The largest difference between experimental and theoretical value is for the N(2A)-Ni(1)-N(5A) and O(1A)-Ni(1)-N(1A) bond angles, 25.99 Å and 49.9 Å respectively. There is an extensive hydrogen bonding network within each layer and between layers. The geometrical parameters of H-bonds are collected in Table S4 (Supplementary data). The two complex molecules are firmly connected by several complicated intermolecular H-bonds in the perchlorate anion, O–H⋯⋯O–Cl and C–H⋯⋯O–Cl, crystalline water molecules and N(6A)–H(6A)⋯⋯O(1W)–H and N(3B)–H(3B)⋯⋯O(2W)–H, thus leading to the formation of two dimensional supra-molecular networking.

To simulate the experimental electronic spectra, TDDFT/B3LYP/LANL2DZ calculations for ligand and complexes (**1**) and (**2**) in DMSO have been carried out. The calculated vertical excitation energies oscillator strength and tentative nature of the transition obtained at the TD-DFT level presented in Table 2, shows three absorptions [$^3A_{2g}\rightarrow{}^3T_{2g}(\nu_1)$, $^3A_{2g}\rightarrow{}^3T_{2g}$(F) ($\nu_2$), $^3A_{2g}\rightarrow{}^3T_{2g}$ (P) (ν_3)] and one weak absorption characteristic of regular octahedral nickel(II) complexes[39]. The absorption band at 320 nm for ligand is due to the six high energy excitations. These excitation states are contribution of βHOMO→βLUMO (49%), βHOMO-1→βLUMO(22%), βHOMO→βLUMO (22%), βHOMO→βLUMO+1(44%), βHOMO-2→βLUMO (40%), βHOMO→βLUMO (22%) and βHOMO-1 →βLUMO (20%) transitions (Supplementary data, Fig. S1). The absorption band at 693 nm for complex (**1**) appears to be contributed by three excitations at 1.0109 eV (1229 nm and f = 0.0001), 1.562 eV (628 nm and f = 0.005) and 1.565 eV (628 nm and f = 0.005), assigned to $^3A_{2g}\rightarrow{}^3T_{2g}$(F) (Fig. 4). Similarly, the band 998 nm for (**1**) is due to the composition of two excitations, 0.698 eV (1380 nm and f = 0.000) and 1.233 eV (959 nm and f = 0.002), which can be attributed to βHOMO-1→βLUMO(44%) and βHOMO-1 →βLUMO+1(23%), assigned to $^3A_{2g}\rightarrow{}^3T_{2g}$/ *d-d* transition. A more intense band at 82 nm is composed of βHOMO→βLUMO (45%) at 1.770 eV (578 nm and f = 0.0027) which may be assigned to $^3A_{2g}\rightarrow{}^3T_{2g}$ (P)/ LMCT/ *d-d* transition.

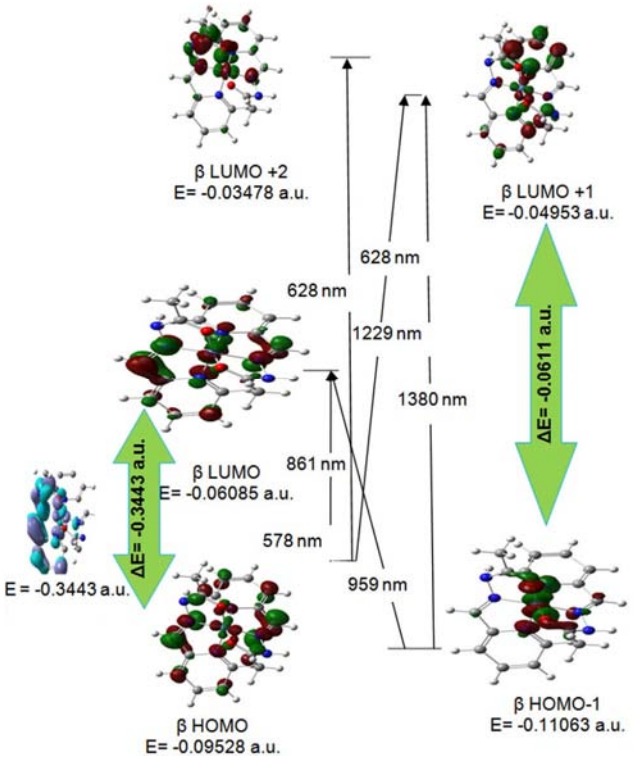

Fig. 4 – Selected orbital excitation of complex (**1**) and their HOMO→ LUMO energy level diagrams.

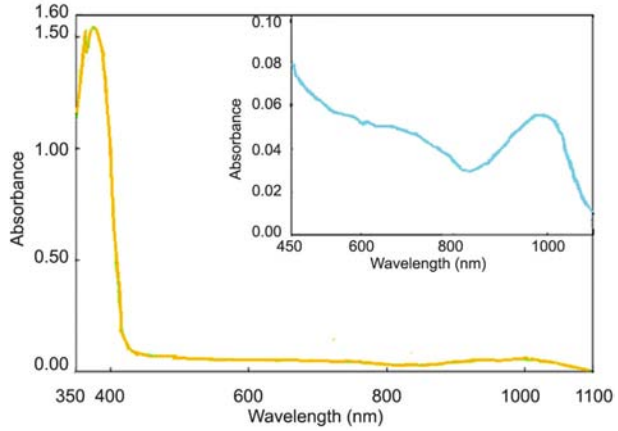

Fig. 5 – UV-visible spectrum of complex (**1**) (0.00025 mol dm^{-3}). [Inset: UV-visible spectrum of complex (**1**) (0.003 mol dm^{-3}).

In complex (**2**), the band at 998 nm appears to be a composition of three excitations at 0.3933 eV (1352 nm and 0.0005), 1.0071 eV (1231 nm and 0.0002) and 1.340 eV (924 nm and 0.0007). These are low energy transitions due to βHOMO→βLUMO (87%), βHOMO→βLUMO+1 (51%), and βHOMO→βLUMO+1 (17%), which may be assigned to *d-d* transitions. Similarly, the band at 680 nm appears to be

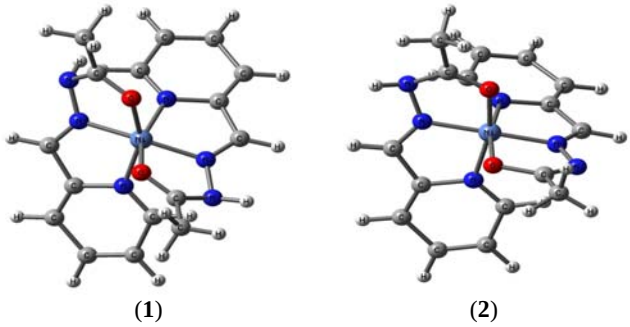

(**1**) (**2**)

Fig. 6 – Optimized structure of complexes (**1**) and (**2**).

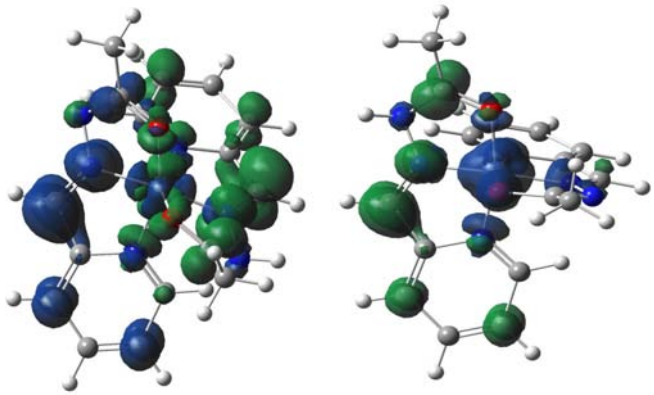

(**1**) (**2**)

Fig. 7 – Spin density plots of complexes (**1**) and (**2**).

composition of two excitations, at 1.341 eV (924 nm and f = 0.007) and 1.4270 eV (868 nm and f = 0.0003) due to the contributions of βHOMO→βLUMO+3 (48%) and βHOMO→βLUMO+3 (15%). These transitions may be assigned to *d-d* transitions. A more intense band at 380 nm is composed of βHOMO→βLUMO+4 (94%). The experimental electronic spectrum of complex (**1**) is shown in Fig. 5.

To understand the electronic structure of complexes (**1**) and (**2**), DFT calculations have been performed. The fully geometry optimization for the compounds (**1**) and (**2**) has been carried out in the DFT/B3LYP level. The optimized bond lengths and bond angles are well reproduced with the X-ray data of the complexes (Tables S1 and S2). The geometries of the (**1**) and (**2**) optimized in the singlet ground state are given in Fig. 6. The LUMO orbitals of (**1**) and (**2**) exhibit a larger number of nodes than the HOMO orbitals. Figure 7 represents the spin density of the unpaired spin distributed over 10% Cu, 5% N and 85% of C atom for (**1**) and 57% Cu, 35% N and 8% of O atom for (**2**), along with major contribution on the nickel center.

Supplementary data

The X-ray crystallographic data for the structures reported herein have been deposited under CCDC No. 1414056 (**1**) and 1414058 (**2**). These data can be obtained free of charge via http://www.ccdc.cam.ac.uk/structure-summary-form the Cambridge Crystallographic Data Centre, 12 Union Road, Cambridge CB2 1EZ, UK; Email: deposit@ccdc.cam.ac.uk . Other supplementary data associated with this article, i.e., Fig. S1 and Tables S1-S4, are available in the electronic form at http://www.niscair.res.in/jinfo/ijca/IJCA_54A(12)1459-1465_SupplData.pdf.

Acknowledgment

The authors wish to acknowledge the assistance of Dr. M Zeller, Youngstown State University, USA, in the collection of diffraction data and NSF Grant CHE 0087210, Ohio Board of Regents Grant CAP-491 and by Youngstown State University, USA, for funds to purchase the X-ray diffractometer. CSIR-Central Drug Research Institute, Lucknow, India, is thankfully acknowledged for providing analytical and spectral facilities. Financial assistance from MP Council of Science & Technology, Bhopal, India, [Scheme No. A/RD/RP-2/2015-16/245] is also acknowledged.

References

1 Sigel H, *Inorg Chem*, 19 (1980) 1411.
2 Stanyon HF, Cong X, Chen Y, Shahidullah N, Rossetti G, Dreyer J, Papamokos G, Carloni P & Viles J H, *FEBS J*, 281 (2014) 3945.
3 Sigel A, Sigel H, Sigel RKO, *Metal Ions in Lifesciences*, Vol. 2, (Wiley, Chichester), 2007.
4 Patel R N, Shukla K K, Singh A, Patel D K & Sondhiya V P, *Trans Met Chem*, 36 (2011) 179.
5 Biswas C, Drew M G B & Ghosh A, *Inorg Chem*, 47 (2008) 4513.
6 Biswas C, Chattopadhyay S, Drew M G B & Ghosh A, *Polyhedron*, 26 (2007) 4411.
7 Murata T, Yakiyama Y, Nakasuji K & Morita Y, *Cryst Growth Des*, 10 (2010) 4898.
8 Scott P & Random L, *J Phys Chem*, 100 (1996) 16505.
9 Denis P & Ventura O N, *J Mol Struct*, 537(2001) 173.
10 Abbowicz-Bienko A J, Bienko D C & Latajka Z, *J Mol Struct*, 552 (2000) 165.
11 Jacob R & Fiscker G, *J Mol Struct*, 613 (2002) 175.
12 Banclersen K, Langgard M & Sparget-Larsen J, *J Mol Struct*, 509 (1999) 153.
13 Song Y Z, Zhou J F, Song Y, Wei Y G & Wang H, *Bioorg Med Chem Lett*, 15 (2005) 4672.
14 Jayabharathi J, Thanikachalam V & Perumal M V, *Spectrochim Acta: A*, 95 (2012) 614.
15 Patel R N, Singh N & Gundla V L N, *Polyhedron*, 26 (2007) 757.
16 Patel R N, Singh A, Shukla K K, Patel D K & Sondhiya V P, *Indian J Chem*, 49A (2010) 1601.
17 Patel R N, Shukla K K, Singh A, Choudhary M, Patel D K, Niclos-Gutierrez J & Choquesillo-Lazarte D, *J Coord Chem*, 63 (2010) 3648.
18 Patel R N, Singh A, Sondhiya V P, Singh Y, Shukla K K, Patel D K & Pandey R, *J Coord Chem*, 65 (2012) 795.
19 Rawat S P, Patel R N & Choudhary M, *J Indian Chem Soc*, 91 (2014) 1079.
20 Datta A, Sheu S C, Liu P H & Huang J H, *Acta Cryst: E*, 67 (2011) 1852.
21 *SADABS*, ver. 2.03, (University of Gottingen, Germany) 2002.
22 SMART (ver. 5.628), SAINT (ver. 6.45a), *XPREP*, *SHELXTL*, (Bruker AXS Inc., Madison, WI, USA) 2004.
23 Sheldrick G M, *Acta Crystallogr: A*, 64 (2008) 112.
24 Spek A L, *Acta Crystallogr: D*, 65 (2009) 148.
25 Farrugia L J, *J Appl Crystallogr*, 30 (1997) 565.
26 Farrugia L J, *WinGX*, *J Appl Crystallogr*, 32 (1999) 837.
27 Gauss View 5.0.9, (Gaussion Inc., Wallingford, CT, USA), 2009.
28 *Gaussian 09, rev. D.01*, (Gaussian, Inc., Wallingford CT, USA) 2013.
29 Dozer D T & Handy N C, *Phys Chem*, 2 (2000) 2117.
30 Hay P J & Wadt W R, *J Chem Phys*, 82 (1985) 270.
31 Geary W J, *Coord Chem Rev*, 7 (1971) 81.
32 Patel R N, *Indian J Chem*, 48A (2009)1370.
33 Elber S R, Helland B J, Jacobson R A & Angilicy R J, *Inorg Chem*, 19 (1980) 175.
34 Battablia L P, Corradi A B, Antolini L, Marcotrigiano G, Menabue L & Pellacani G C, *J Am Chem Soc*, 104 (1982) 2407.
35 Chandra S & Gupta L K, *Spectrochim Acta*, 60 (2004) 1751.
36 Jana S, Bhaumik P K, Harms K & Chattopadhyay S, *Polyhedron*, 78 (2014) 94.
37 Marsh J, *Advanced Organic Chemistry, Reaction Mechanisms and Structure*, 4th Edn, (Wiley, New York) 1992.
38 Chaviara A T, Cox P J, Repana K H, Pantazaki A A, Papazisis K T, Kortsaris A H, Kyriakidis D A, Nikolov G S & Bolos C A, *J Inorg Biochem*, 99 (2005) 467.
39 Drago R S, Meek D W, Joesten M D & Laroche L, *Inorg Chem*, 2 (1963)124.